Original article

Nuclear Medicine Communications

Reverse perfusion pattern in myocardial perfusion imaging using technetium-99m-sestamibi in patients with intermediate risk for coronary artery disease in relation to the time of acquisition and intensity of visceral uptake as artifactual causes

Babak Fallahi[a], Davood Beiki[a], Yalda Salehi[a], Alireza Emami-Ardekani[a], Armaghan Fard-Esfahani[a], Farahnaz Aghahosseini[a], Mahdi Haghighatafshar[b] and Mohammad Eftekhari[a]

Objective **With respect to the equivocal value of the reverse perfusion pattern (RPP) in technetium-99m (^{99m}Tc)-sestamibi myocardial perfusion imaging, a study was carried out to evaluate this pattern in association with the presence or absence of coronary artery disease (CAD) and other underlying factors, mainly the time of acquisition and the presence of intense visceral uptake.**

Patients and methods **We prospectively studied 102 patients with a moderate risk of CAD (41 men and 61 women, mean age: 56.5 ± 9.2 years) without a previous history of documented CAD, myocardial infarction, or revascularization. Myocardial perfusion imaging was performed using a 2-day dual-phase protocol with the stress and rest images, each obtained 15, 120, and 180 min after an injection of 666–814 MBq ^{99m}Tc-MIBI. According to the time of image acquisition, the following five protocols were defined, A: 15/15 min, B: 15/180 min, C: 180/180 min, D: 180/15 min, and E: 120/120 min for stress/rest images, respectively.**

Results **The odds of RPP were higher in the cases with more intense infradiaphragmatic visceral uptake on rest-phase images of the protocols A and D (odds ratios = 1.2–7.8 and 1.2–7.5, respectively). Our results showed that RPP is related to incorrect normalization. Also, diabetes, sex, and CAD did not correlate with RPP.**

Conclusion **This study found no relationship between RPP and CAD, diabetes mellitus, and sex; however, an association was found between RPP and incorrect normalization because of the variation of visceral uptake intensity in relation to the time of acquisition at stress and rest phases favoring the artifactual base of this pattern.** ***Nucl Med Commun*** **38:15–20** **Copyright © 2016 Wolters Kluwer Health, Inc. All rights reserved.**

Nuclear Medicine Communications 2017, **38**:15–20

Keywords: myocardial perfusion imaging, reverse perfusion, technetium-99m-sestamibi

[a]Research Center for Nuclear Medicine, Shariati Hospital, Tehran University of Medical Sciences, Tehran and [b]Nuclear Medicine and Molecular Imaging Research Center, Namazi Teaching Hospital, Shiraz University of Medical Sciences, Shiraz, Iran

Correspondence to Yalda Salehi, MD, Research Center for Nuclear Medicine, Shariati Hospital, Tehran University of Medical Sciences, North Kargar Ave., Tehran 1411713135, Iran
Tel/fax: +98 21 6691 9588; e-mail: salehi_y@sina.tums.ac.ir

Received 11 January 2016 **Revised** 18 July 2016 **Accepted** 13 September 2016

Introduction

Reverse perfusion pattern (RPP) in myocardial perfusion imaging (MPI) is an at-rest perfusion defect in a myocardial territory showing normal perfusion on stress images or a worsening of a pre-existing stress-induced perfusion defect on the rest images. RPP with thallium-201 imaging has been well documented and explored in depth, and is called the reverse redistribution (RR) phenomenon [1–3]. Some investigators have also defined a similar pattern for technetium-99m (^{99m}Tc)-labeled radiotracers in some cases; however, its mechanism and significance still remain unclear [4–13]. Some studies have described a relationship between RPP and myocardial damage, metabolic dysfunction of myocytes, and ischemia or viability because of coronary artery disease (CAD) [4,5,7,8,12]. In addition, other studies have reported this pattern to be observed predominantly in recent myocardial infarction (MI), chronic stable CAD, and some other disorders such as X-syndrome, sarcoidosis, Chagas disease, and post-transplantation condition [14,15], whereas in some others, RPP frequently occurred in patients with a low risk of CAD as an artifactual finding and has been assumed to be clinically unimportant [6,13–14].

The exact mechanism of RPP in MPI using technetium-99m methoxy isobutyl isonitrile (^{99m}Tc-MIBI) has not been well characterized as yet. However, a mechanism similar to that of the thallium-201 RR phenomenon may also occur with ^{99m}Tc-sestamibi. Although early redistribution is not shown with ^{99m}Tc-sestamibi MPI, recent

0143-3636 Copyright © 2016 Wolters Kluwer Health, Inc. All rights reserved.

DOI: 10.1097/MNM.0000000000000601

Copyright © 2017 Wolters Kluwer Health, Inc. All rights reserved.

evidence may suggest some degrees of delayed redistribution for this agent [16]. On the basis of this fact, a possible mechanism for reverse perfusion of ^{99m}Tc-sestamibi might be suggested in patients with a history of MI similar to that described for thallium-201. The infarcted myocardium may take up ^{99m}Tc-sestamibi early following a radiotracer injection because of a hyperemic effect after revascularization or thrombolysis. The radiotracer would then be washed out from the infarcted myocardium and redistributed to the viable myocardial zones. In a study on patients who underwent a percutaneous coronary intervention following acute MI, the presence of RR from 1-h to 3-h images was associated with improvement in regional wall motion, confirming viability in the sites of previous MI [5]. This proposed mechanism, albeit reasonable for patients with a history of MI or documented chronic CAD, cannot be applied for many cases with a low to intermediate risk of CAD without evidence of a previous cardiac event referred just for diagnostic purposes.

In another study, the difference in the myocardial and extramyocardial visceral uptake with the variation of acquisition time in a dual-phase MPI resulted in different image quality and MPI accuracy. This may be because of ^{99m}Tc-sestamibi dynamic changes over time in the myocardium [17]. Thus, the time of acquisition may also influence the rate of RPP in a ^{99m}Tc-sestamibi MPI.

In terms of the controversial hypotheses about the causes of RPP, this study aimed to evaluate RPP and its relation to various factors including sex, presence versus absence of diabetes mellitus, type of stress protocol (pharmacologic vs. exercise), and the time elapsed from ^{99m}Tc-sestamibi injection to the onset of MPI acquisition. In addition, to assess the value of this pattern in the diagnosis of CAD, the association between documented coronary artery stenosis and the presence of RPP was evaluated in a subgroup of patients with a moderate pretest probability of CAD.

Patients and methods

In this prospective study, 102 consecutive patients with a moderate risk of CAD were enrolled, most of them referred for the evaluation of acute chest pain or risk stratification before nonvascular surgery. All patients had an intermediate pretest probability of CAD according to the Framingham Risk Score, without any history of severe obstructive pulmonary disease, MI, or echocardiographic evidence of cardiomyopathy. The study was approved by the Ethical Committee of Tehran University of Medical Science.

Patient preparation

After obtaining written informed consent, all patients were fasted for at least 4 h before the stress phase. Consumption of nitrates, β blockers, and calcium blocker drugs was not allowed up to 24 h before the exercise stress test. Caffeine-containing foods or drugs and long-acting aminophylline were discontinued 24 h before the dipyridamole stress test.

Image acquisition sequence

A commercial ^{99m}Tc-sestamibi kit (AEOI, Tehran, Iran) was used to provide ^{99m}Tc-MIBI for MPI. The gated MPI was performed after an injection of 666–814 MBq ^{99m}Tc-MIBI on the basis of the patient's weight at peak treadmill exercise (31 cases) or following a dipyridamole infusion (71 cases). For the treadmill exercise, the Bruce protocol was used and the radiotracer was injected at peak exercise. The exercise continued for a minimum of 60–90 s after radiotracer injection. The standard pharmacological stress was performed with an intravenous injection of 0.56 mg/kg dipyridamole over a 4-min period. Stress MPI was carried out at 15, 120, and 180 min after the injection of 666–814 MBq ^{99m}Tc-MIBI. All images were obtained using a dual-head SPECT gamma camera (ADAC Solus; ADAC Laboratories, Milpitas, California, USA), equipped with low-energy, high-resolution collimators, with a 15% energy window around the 140 keV photo-peak. Patients were positioned supine. Images were acquired using a 64×64 matrix within a 38.5 cm detector mask over a 180° rotation arc in a step and shoot method for 32 projections, each lasting 30 s, from 45° right anterior oblique to 45° left posterior oblique views. The rest study was carried out with a similar dose of radiotracer activity, imaging protocol, and at the same time intervals on the following day.

Image analysis

Five sets of image reconstructions were defined as protocols A to E. In protocol A, the stress images from the 15-min acquisition and rest images from 15-min acquisition (15/15) were used. In addition, protocol B for 15/180, protocol C for 180/180, protocol D for 180/15, and protocol E for 120/120 min stress/rest acquisitions were applied for visual and semiquantitative assessments. The raw images were reconstructed using a Ramp and Butterworth filtered back projection and demonstrated in short-axis, vertical long-axis, and horizontal long-axis views. Two expert nuclear medicine physicians visually reviewed the images on the basis of the standard 20-segment model. Each setting of images was evaluated separately and the corresponding results were recorded independently such that for each protocol, the observers were unaware of their interpretations for the other protocols. In addition, a semiquantitative image analysis was carried out for each protocol using QPS/QGS AutoQUANT software (ADAC Laboratories). Summed stress score, summed rest score, and summed difference score were estimated using this software. The visceral activity was compared with the myocardial uptake on the basis of visual assessment and the results were confirmed by a semiquantitative evaluation. For this reason, regions of interest (ROIs) were drawn around the myocardium as well as the subdiaphragmatic region with the maximum

Copyright © 2017 Wolters Kluwer Health, Inc. All rights reserved.

Fig. 1

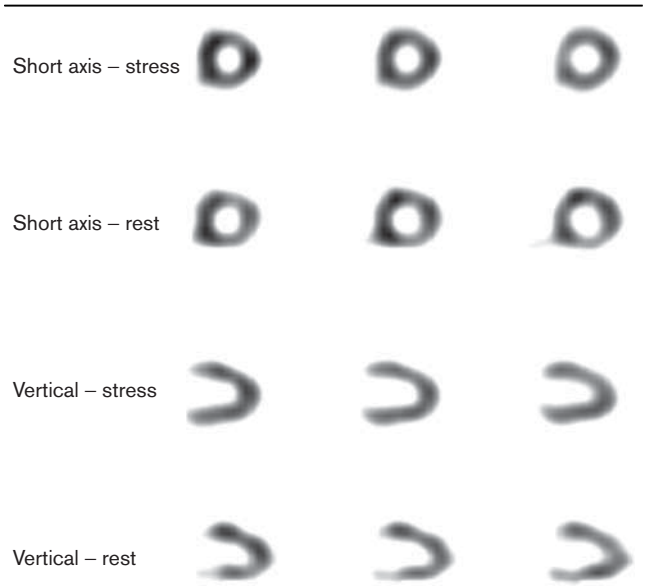

Reverse pattern of perfusion in the inferior myocardial wall on stress/rest technetium-99m-sestamibi images.

intensity of uptake. The maximum intensity of visceral uptake (either in the hepatic or the gastrointestinal region) was correlated with the maximum intensity of uptake in the myocardium and, correspondingly, the intensity of visceral uptake was classified into two categories – that is, 'equal to or more than myocardium' versus 'less than myocardium'. RPP-a is defined as an at-rest perfusion defect in a myocardial territory showing normal perfusion on stress images (Fig. 1) and RPP-b is identified as worsening of a pre-existing stress-induced perfusion defect on the rest images.

Follow-up evaluations

All patients were observed in a follow-up program for at least a 1-year period. All soft events including angina pectoris or invasive and noninvasive diagnostic and interventional procedures such as revascularization, as well as any 'hard' cardiac events such as deaths that are attributed to CAD or nonfatal MI were recorded during follow-up period. Coronary angiography was performed for 35 (34.3%) patients within this period and the findings were reported by consensus of two expert cardiologists who were blinded to the results of MPI. Significant CAD was defined as at least 50% stenosis in one or more main coronary arteries or their major branches.

Statistical analysis

The commercial software SPSS (v. 17.0; SPSS Inc., Chicago, Illinois, USA) was used for statistical analysis. Numeric variables with a normal distribution (such as age) were described as mean ± SD. Cross-tabulation and the χ^2-test were used for univariate analysis of the association between nominal variables. The Fisher exact test was used when the 2×2 crosstab has a cell with an expected frequency of less than 5. The odds ratios (ORs) with 95% confidence interval were also calculated. P values less than 0.05 were considered statistically significant.

Results

We studied 102 (41 men and 61 women) patients with a mean age of 56.5 ± 9.2 years. The frequencies of RPP in different protocols were as follows: 31 (30.4%) in protocol A, 32 (31.4%) in protocol B, 31 (30.4%) in protocol C, 43 (42%) in protocol D, and 21 (20.6%) in protocol E.

The frequencies and ORs of RPP in relation to the intensity of visceral uptake for each protocol are summarized in Table 1. The frequencies of the two different patterns of RPP are shown separately; however, because of the low frequency of RPP-b, the OR analyses are carried out on the basis of the total number of patients showing RPP. As noted in this table, the frequency of intense visceral uptake and consequently the ORs of RPP are significantly higher when the rest-phase imaging is performed early after an injection of radiotracer (protocols A and D). Conversely, the frequency of visceral uptake is minimal when the rest phase is markedly delayed (only 2% in protocol B, C, and E).

However, the summarized results of stress images in Table 2 show that the ORs of RPP in patients with visceral uptake intensity more than myocardium versus those with visceral uptake less than myocardium are significantly decreased when the stress phase is performed early after radiotracer injection, whereas the rest phase is considerably postponed (protocol B, $P = 0.008$). The intensity of visceral uptake at the stress phase shows no remarkable effect on the likelihood of RPP in any other acquisition protocols (Table 2).

Table 3 shows the frequencies of RPP in different myocardial walls on the basis of different protocols. The RPP is observed more frequently in protocols A and D, especially in the activity of the inferior wall.

Univariate analysis showed no significant association between RPP and baseline variables including sex, history of diabetes mellitus, and type of stress (exercise vs. pharmacologic) in protocols A, C, D, and E (Table 4). Also, no association was found between the frequency of RPP in protocol B and sex or history of diabetes mellitus; however, the frequency of RPP using protocol B is significantly lower in patients with dipyridamole versus exercise stress test (25 vs. 45%, $P = 0.047$, Table 4).

In all five protocols applied, the frequency of RPP was not different between the patients diagnosed prospectively with CAD and those confirmed to have normal coronary arteries during the course of follow-up (Table 5).

Copyright © 2017 Wolters Kluwer Health, Inc. All rights reserved.

Table 1 Frequency and odds ratio of reverse perfusion pattern on the basis of visceral radiotracer uptake at the rest phase for each protocol of acquisition

	Uptake intensity less than myocardium			Uptake intensity equal to or more than myocardium				
Protocols	*N* (%)	RPP-a [*n* (%)]	RPP-b [*n* (%)]	*N* (%)	RPP-a [*n* (%)]	RPP-b [*n* (%)]	OR (95% CI)	*P*, significance
A	73 (71.5)	16 (21.9)	2 (2.7)	29 (28.5)	11 (37.9)	3 (10.3)	3.1 (1.2–7.8)	0.014, S
B	100 (98.0)	30 (30)	2 (2)	2 (2.0)	1 (50)	0 (0)	2.2 (0.1–35.7)	0.540, NS
C	100 (98.0)	29 (29)	2 (2)	2 (2.0)	0 (0)	0 (0)	[a]	1.000, NS
D	74 (72.5)	26 (35.1)	1 (1.4)	28 (27.5)	15 (53.6)	3 (10.7)	3.0 (1.2–7.5)	0.015, S
E	100 (98.0)	19 (19)	1 (1)	2 (2.0)	1 (50)	0 (0)	3.9 (0.2–65.9)	0.374, NS

CI, confidence interval; OR, odds ratio of reverse perfusion pattern (a or b) for the patients with visceral uptake intensity of more than myocardium versus those with less than myocardium; RPP-a, reverse perfusion pattern with normal stress perfusion and decreased perfusion pattern on rest images; RPP-b, worsening of a pre-existing stress-induced perfusion on rest images; S, significant.
[a]The odds ratio could not be calculated because of a frequency of 0 in at least one cross-tabulation cell.

Table 2 Odds ratios of reverse perfusion pattern in relation to the intensity of visceral uptake at the stress phase for each protocol of acquisition

Protocols	OR (95% CI)	*P*, significance
A	0.45 (0.17–1.19)	0.115, NS
B	0.27 (0.1–0.75)	0.008, S
C	[a]	1.000, NS
D	[a]	0.504, NS
E	8.3 (0.7–96.5)	0.109, NS

CI, confidence interval; OR, odds ratio of reverse perfusion pattern for the patients with visceral uptake intensity of more than myocardium versus those with less than myocardium at the stress phase; S, significant.
[a]The odds ratio cannot be calculated because of a frequency of 0 in at least one cross-tabulation cell.

Table 3 The frequency of reverse perfusion pattern in different myocardial walls on the basis of the acquisition protocol

	Myocardial wall [*n* (%)]				
Protocols	Anterior	Inferior	Lateral	Septal	Apical
A	16 (16.3)	20 (20.4)	11 (11.2)	12 (12.2)	10 (10.2)
B	17 (16.7)	15 (14.7)	8 (8)	11 (11)	14 (16.3)
C	16 (15.7)	14 (13.7)	4 (3.9)	8 (7.8)	12 (11.8)
D	20 (20.2)	28 (28.3)	11 (11.1)	15 (15.2)	19 (19.2)
E	10 (9.8)	9 (8.8)	5 (4.9)	7 (6.9)	6 (5.9)

Table 5 Comparison between the frequencies of reverse perfusion pattern in coronary artery disease versus normal coronary cases in five different protocols

	Frequency of cases with reverse perfusion pattern [*n* (%)]			
Protocols	Coronary stenosis (*N* = 20)	Normal coronary (*N* = 15)	Total (*N* = 35)	*P*, significance of difference
A	6 (30)	5 (33.3)	11 (31.4)	0.833, NS
B	8 (40)	5 (33.3)	13 (37.1)	0.686, NS
C	6 (30)	5 (33.3)	11 (31.4)	0.833, NS
D	9 (45)	9 (60)	18 (51.4)	0.380, NS
E	4 (20)	4 (26.7)	8 (22.9)	0.642, NS

Discussion

The present study evaluated perfusion scanning in two different rest and stress phases. In general, dual-phase MPI provides information for myocardial perfusion impairment. In a radionuclide MPI, RPP is defined as a new perfusion defect at rest that is not detectable on stress images or worsening of a pre-existing stress-inducible defect on the rest images. The incidence of RPP in previous studies varies from 5 to 38% [8–11]. Our study was in line with previous surveys, with RPP frequency ranging from 20.6% using a routine protocol (E) up to 42% using protocol D in which the stress phase was delayed for at least 3 h and the rest phase was obtained within a short time (as early as 15 min) after radiotracer injection.

Although the cause of RPP is unknown, the wide range of RPP frequencies in different stress and rest acquisition time settings may be a remarkable indicator of procedure-

Table 4 The proportional frequency of reverse perfusion pattern on the basis of baseline factors in different acquisition protocols

		Protocol [*n* (%)]									
		A		B		C		D		E	
Factors	*N*	RPP freq.	*P*, sig.	RPP freq.	*P*, sig.	RPP freq.	*P*, sig.	RPP freq.	*P*, sig.	RPP freq.	*P*, sig.
Sex											
Female	61	21 (34.4)	0.201, NS	19 (31.1)	0.952, NS	17 (27.9)	0.499, NS	27 (44.3)	0.621, NS	15 (24.6)	0.223, NS
Male	41	10 (24.3)		13 (31.7)		14 (34.1)		16 (39.0)		6 (14.6)	
History of diabetes mellitus											
Yes	28	9 (32.1)	0.813, NS	12 (42.8)	0.124, NS	9 (32.1)	0.813, NS	13 (46.4)	0.527, NS	6 (21.4)	0.897, NS
No	74	22 (29.7)		20 (27.0)		22 (29.7)		30 (40.5)		15 (20.3)	
Type of stress											
Exercise	31	11 (35.5)	0.460, NS	14 (45.2)	0.047, S	11 (35.5)	0.460, NS	11 (35.5)	0.367, NS	6 (19.4)	0.839, NS
Dipyridamole	71	20 (28.2)		18 (25.4)		20 (28.2)		32 (45.1)		15 (21.1)	

RPP freq, proportional frequency of reverse perfusion pattern; sig, significance (*P* value) for the difference of the reverse perfusion pattern on the basis of variable factors.

Copyright © 2017 Wolters Kluwer Health, Inc. All rights reserved.

related factors contributing toward the creation of this pattern. However, some studies explain that RPP may be associated with the real changes in myocardial perfusion, especially in patients with a history of chronic ischemic heart disease [12,18]. Also, RPP may be related to dilatation of collateral circulation induced by stress or a partially stenotic coronary artery supplying damaged but viable myocardium [4,10]. Moreover, RPP could also be described by a stress-induced hyperemia of viable myocardium following revascularization in patients with acute MI [2,5,7].

In a study, ^{99m}Tc-sestamibi images were compared between 1-h (early) and 3-h (delayed) images, concluding that rapid washout from the myocardium on delayed images is the main cause of RPP, indicating the patency of infarct-related artery and a preserved myocardial viability that was confirmed by recovery of left ventricular function following revascularization [5]. This association has also been confirmed by other research [7]. Moreover, Tejeda *et al.* [9] noted that RPP is more prevalent in patients with low ejection fraction and MI. In addition, some studies have shown that RPP may be related to CAD accompanied by diabetes [9], whereas others did not confirm any association between RPP and diabetes, dyslipidemia, or smoking [18]. No association was also found between RPP and CAD, diabetes mellitus, and sex in our study.

In contrast to our study, the above-mentioned studies have mostly been carried out in patients with a previous or a recent history of MI with or without revascularization to assess the value of RPP in association with post-MI viability. However, in these studies, the value of RPP has not been reported in the diagnosis of ischemia in patients without any history of documented CAD, revascularization, or previous MI. To our knowledge, the current study is the first in which RPP was assessed in different sets of images to evaluate RPP in variable acquisition times. The study results may significantly aid improvement in MPI accuracy for the diagnosis of ischemia in intermediate-risk patients without any history of documented CAD or MI. Our results not only show no association between RPP and documented CAD but also show a significant relationship between the RPP and the intensity of visceral uptake at the rest phase, especially when the rest-phase images were obtained in a short time following radiotracer injection (protocols A and D). The higher the visceral uptake on the early-phase rest images, the more frequently RPP is evident. Conversely, the OR of RPP in the patients showing higher visceral uptake than myocardium versus those with lower visceral uptake on the stress images was significantly decreased when the stress acquisition was obtained earlier (by 15 min) and the rest-phase imaging was delayed for at least 3 h (significant OR in protocol B from 0.1 to 0.75 compared with insignificant OR in the other protocols). These findings may be a result of incorrect normalization of the whole myocardium in reference to intense extracardiac activity not adequately cleared from the subdiaphragmatic region during the limited time of washout after radiotracer injection at the rest phase. The higher frequency of RPP in the inferior wall and the lower frequency of this pattern in the lateral wall as noted in our study may justify this theory. Similar frequencies of RPP in the inferior and lateral walls have also been reported previously [18], corresponding to the fact that the inferior wall is the most common region of incorrect normalization (ramp filter effect) and the lateral wall is rarely the site of this artifact.

The effect of scatter from bowel or liver activity on the frequency of RPP has also been explained by other investigators [2]. In addition, some authors suggested that RPP may be more frequent in obese patients with abdominal protuberance, in women with large and dense breasts, in those who underwent a 1-day protocol with a higher stress dose of radiotracer and count-density in comparison with the rest phase, and even in patients for whom the attenuation correction algorithm was applied, confirming the artifactual nature of this pattern [2,6,14].

Time difference in acquisitions in different protocols does not represent a significant drawback in our study because all image projections are normalized to the maximum intensity pixel of the same phase images. In fact, the concept of normalization in MPI is to adjust the imaging data so that a direct comparison can be performed even when data sets are acquired at different times with different tracer doses. However, the analyses are not on the basis of absolute quantification that is influenced by the radiotracer decay, whereas count ratio analyses, like visual assessment of the images, are not influenced by the radiotracer decay.

Early stress imaging, in addition to lower frequency of artifactual RPP, is associated with higher sensitivity to detect the perfusion abnormalities probably as a result of minimal redistribution of ^{99m}Tc-sestamibi on delayed stress images [17,19] and a higher detection rate of poststress myocardial stunning as a prognostic marker of CAD [19].

Conclusion

Despite former suggestions in favor of the association between RPP and myocardial viability in patients with previous MI with or without a history of revascularization, this phenomenon is of limited value for detecting CAD cases among patients with intermediate pretest probability referred for diagnostic purposes. RPP in these cases is more likely related to the artifactual causes resulting from the incorrect normalization because of variation in visceral uptake on the stress versus rest images caused by different acquisition times in a dual-phase MPI. This pattern is most likely observed when the rest-phase imaging is performed soon after injection,

Copyright © 2017 Wolters Kluwer Health, Inc. All rights reserved.

whereas it is less observed when the stress-phase imaging is performed early after injection.

Acknowledgements

This study is part of an MD thesis and supported by Tehran University of Medical Sciences, Tehran, Iran (grant no. 9847).

Conflicts of interest

There are no conflicts of interest.

References

1 Pace L, Cuocolo A, Maurea S, Nicolai E, Imbriaco M, Nappi A, *et al*. Reverse redistribution in resting thallium-201 myocardial scintigraphy in patients with coronary artery disease: relation to coronary anatomy and ventricular function. *J Nucl Med* 1993; **34**:1688–1692.
2 Yong-Ming H, Xiang-Jun Y. Microcirculation dysfunction: a possible mechanism responsible for reverse redistribution in myocardial perfusion imaging? *Curr Med Imaging Rev* 2009; **5**:197–202.
3 Arrighi JA, Soufer R. Reverse redistribution: is it clinically relevant or a washout? *J Nucl Cardiol* 1998; **5**:195–201.
4 Shih W, Miller K, Stipp V, Maqour S. Reverse redistribution on dynamic exercise and dipyridamole stress technetium-99m-MIBI myocardial SPECT. *J Nucl Med* 1995; **36**:2053–2055.
5 Takeishi Y, Sukekawa H, Fujiwara S, Ikeno E, Sasaki Y, Tomoike H. Reverse redistribution of technetium-99m-sestamibi following direct PTCA in acute myocardial infarction. *J Nucl Med* 1996; **37**:1289–1294.
6 Kao CH, Wang SJ, Ting CT, Chen YT. 'Reverse redistribution pattern' during myocardial perfusion imaging with Tc-99m-MIBI. *Nucl Med Commun* 1996; **17**:397–399.
7 Fujiwara S, Takeishi Y, Atsumi H, Yamaki M, Takahashi N, Yamaoka M, *et al*. Prediction of functional recovery in acute myocardial infarction: comparison between sestamibi reverse redistribution and sestamibi/BMIPP mismatch. *J Nucl Cardiol* 1998; **5**:119–127.
8 Sugihara H, Taniguchi Y, Kinoshita N, Nakamura T, Hirasaki S, Azuma A, *et al*. Reverse redistribution of Tc-99m-tetrofosmin in exercises myocardial SPECT in patients with hypertrophic cardiomyopathy. *Ann Nucl Med* 1998; **12**:287–292.
9 Orea-Tejeda A, Castillo-Martinez L, Armando Aguilar-Sáenz C, Asensio-Lafuente E, Corzo-Leon D, Narvaez-David R, *et al*. Reverse redistribution phenomenon in patients with normal coronary epicardial arteries and its relationship to systolic left ventricular dysfunction. *Intern J Cardiol* 2005; **4**:1.
10 Fragasso G, Chierhia S, Dosio F, Pizzetti G, Gianolli L, Fazio F. Reverse perfusion pattern of Tc-99m heralding the development of myocardial infarction. *Clin Nucl Med* 1996; **21**:519–522.
11 Sugihara H, Kinoshita N, Adachi Y, Taniguchi Y, Ohtsuki K, Azuma A, *et al*. Early and delayed Tc-99m-tetrofosmin myocardial SPECT in patients with LBBB. *Ann Nucl Med* 1998; **12**:281–286.
12 Tanaka R, Nakamura T, Chiba S, Ono T, Yoshitani T, Miyamoto A, Yamazaki J. Clinical implication of reverse redistribution on ^{99m}TC-sestamibi images for evaluating ischemic heart disease. *Ann Nucl Med* 2006; **20**:349–356.
13 Meka M, DePuey GE. Apparent reverse distribution of Tc-99m sestamibi on myocardial perfusion scan. *J Nucl Cardiol* 2007; **14**:e11–e14.
14 Araujo W, DePuey EG, Kamran M, Undavia M, Friedman M. Artifactual reverse distribution pattern in myocardial perfusion SPECT with technetium-99m sestamibi. *J Nucl Cardiol* 2000; **7**:633–638.
15 Sekhri V, Sanal S, Delorenzo LJ, Aronow WS, Maguire GP. Cardiac sarcoidosis: a comprehensive review. *Arch Med Sci* 2011; **7**:546–554.
16 Beiki D, Fallahi B, Mohseni Z, Khalaj A, Fard-Esfahani A, Eftekhari M. Initial and delayed stress phase imaging in a single-injection double-acquisition SPECT. The potential value of early ^{99m}Tc-MIBI redistribution in assessment of myocardial perfusion reversibility in patients with coronary artery disease. *Nuklearmedizin* 2010; **49**:19–27.
17 Fallahi B, Haghighatafshar M, Farhoudi F, Salehi Y, Aghahosseini F. Comparative evaluation of the diagnostic accuracy of ^{99m}Tc-sestamibi gated SPECT using five different sets of image acquisitions at stress and rest phases for the diagnosis of coronary artery disease. *Am J Nucl Med Mol Imaging* 2013; **4**:10–16.
18 Schillaci O, Tavolozza M, Di Biagio D, Lacanfora A, Chiaravalloti A, Palombo E, *et al*. Reverse perfusion pattern in myocardial SPECT with ^{99m}Tc-SestaMIBI. *J Med Life* 2013; **6**:349–354.
19 Dizdarevic S, Singh N, Nair S, de Belder A, Ryan N, Aplin M, *et al*. Early gated SPECT adenosine myocardial perfusion imaging may influence the therapeutic management of patients with coronary artery disease. *Nucl Med Commun* 2015; **36**:386–391.

Copyright © 2017 Wolters Kluwer Health, Inc. All rights reserved.